Research Paper

Detection of the Presence of Rail Corrugation Using Convolutional Neural Network

Maciej TABASZEWSKI[1] ⓘ, Bartosz FIRLIK[2] * ⓘ

[1] *Institute of Applied Mechanics, Poznan University of Technology*
Poznań, Poland; e-mail: maciej.tabaszewski@put.poznan.pl

[2] *Institute of Transport, Poznan University of Technology*
Poznań, Poland

*Corresponding Author e-mail: bartosz.firlik@put.poznan.pl

Rail corrugation is a significant problem not only in heavy-haul freight but also in light rail systems. Over the last years, considerable progress has been made in understanding, measuring and treating corrugation problems also considered a matter of safety.

In the presented research, convolutional neural networks (CNNs) are used to identify the occurrence of rail corrugation in light rail systems. The paper shows that by simultaneously measuring the vibration and the sound pressure, it is possible to identify the rail corrugation with a very small error.

Keywords: corrugation; vibration and noise; machine learning; convolutional networks.

1. INTRODUCTION

Rail corrugation is a (quasi-) sinusoidal wavy wear of the rail surface. It appears as peaks of a bright metallic lustre and darker colour troughs of the depth of a few tenths of a millimetre. Light bands correspond to the presence of a harder material. The parameters characterising the corrugation are wavelength λ (distance between peaks) and the wave amplitude (depth) A. Depending on the wavelength, the standard [1] distinguishes between corrugation with short waves ($\lambda = 30 \div 100$ mm), medium waves ($\lambda = 100 \div 300$ mm) and long waves ($\lambda > 300$ mm). An example of short-pitch corrugation in light rail systems is shown in Fig. 1.

Rail corrugation has been known for at least the last 100 years, but for a long time was considered an enigmatic phenomenon due to the fact that measured corrugation wavelength did not relate to existing wear models.

FIG. 1. An example of short-pitch corrugation in light rail systems.

Nowadays, it is already known that rail corrugation is caused by a great range of dynamic processes, which have been widely discussed in the literature over the last decades [2–12]. One of the first complex researches concerning this phenomenon was conducted by GRASSIE [3, 5–8]. He points to the second torsional resonance of powered wheelsets and the 'pinned-pinned resonance' of the rail as the main causes of corrugation. The resonance of the unsprung mass of the vehicle on the track stiffness is also considered a common cause of corrugation in a wide variety of circumstances, particularly if there is a coincidence of the P2 resonance (associated with the resonance of the vehicle as an unsprung mass on the track stiffness, typically close to the Hertz contact resonance) and the first torsional resonance of the wheelsets [8]. That is why wavy wear is commonly identified in the areas where the road encloses tram rails due to the excessive stiffness of the track (soft rail pads reduce the development of wavy wear) [2].

The type and method of processing rail steel in steelworks during the rail rolling, as well as the inhomogeneous structure of the rail steel material (presence of decarburised places of lower hardness), are also often indicated as the causes of corrugation [4]. Corrugation is also produced by the uniform movement of the same types of trains with little differences in speed.

Since the beginning of the 20th century, rail corrugation has been a significant problem not only in heavy-haul freight, but also in light rail systems [13]. If left uncontrolled, it significantly increases the vibrations affecting the vehicle, as well as the noise emitted to the environment – which can be higher by up to 15 dB (A-weighted sound level) [4]. Due to this high noise level, corrugations are often referred to as 'roaring rails'. This is especially important in tram networks, which often run in a highly urbanised environment, as shorter-pitch corrugation causes

vibrations in the range of the acoustic band perceived by the human ear. Due to the increased contact forces between the wheel and the rail, corrugation causes an increased probability of damage to the rail zone in built-up tracks (cracks, surface defects), damage to bogies (play in screw connections) and increased wear of tram wheelsets. It is also associated with the formation of particular types of rolling contact fatigue (RCF), such as squats and Belgrospi's defect.

Over the last few years, considerable progress has been made not only in understanding but also in measuring and treating corrugation problems, because mitigating corrugation problems is also considered as it is a concern of safety.

The most common detection method of railway track corrugation is based on time-frequency analysis by using bogie or axle box acceleration measurements. An example of such an approach, based on the continuous wavelets analysis and the feature modes from the empirical mode decomposition method (EMD), can be found in [14] in which a coupling dynamics model was developed by using the SIMPACK multibody software. A similar model-based approach was presented in [15] using the wavelet packet energy entropy (WP-EE) or in [16] using the ensemble empirical mode decomposition (EEMD) to estimate corrugation wavelength, then bispectrum features were extracted to recognize the depth with a support vector machine (SVM). In [17], ZHANG et al. proposed a corrugation detection method using the variational mode decomposition method (VMD), combined with the smooth pseudo Wigner-Ville distribution (SPWVD) signal time-frequency analysis method to determine the wavelength and the location of the corrugation. In [18], XIAO et al. proposed corrugation detection and classification using a machine learning approach. The axle box acceleration signal was decomposed by wavelet packet decomposition (WPD) and the subsignals were analysed using an adaptive short-time Fourier transform (ASTFT) to obtain the optimal resolution time-frequency distribution and compute the corresponding entropy. The training and testing samples were classified using an SVM.

In addition to vibroacoustic methods, techniques based on scanning the rail surface are also commonly used. In [19], KANG et al. proposed a corrugation detection method based on laser imaging techniques, using multiple sensors in parallel at high sampling frequency to capture the rail profile. In [20], LI et al. used a 3D rail scanner to analyse the flatness of the rail surface and detect corrugation using the time-frequency analysis based on the wavelet approach.

The measurement methods also include visual assessment (identification of wear based on observing light and dark places on the running surface of the rail head). Increasingly, deep learning methods are used, enabling to obtain precise results despite challenging conditions, such as deteriorated and changeable lighting environments and various types of complex rail surface defects. Recently, classification methods using complex deep convolutional neural networks (CNNs) have become popular in corrugation detection and classification [21].

This article proposes the implementation of CNNs in a supervised-learning system (a classifier) for identifying sections with the occurrence of corrugation based on vibration and acoustic signals. This solution allows to detect corrugation while a vehicle (tram or train) equipped with vibration acceleration sensors and microphones is moving on a track. In this research, we focus only on short-pitch rail corrugation measurements, which are the dominant form of corrugation in Polish railway and tram tracks.

2. CLASSIFICATION USING CNNs

A classifier is a supervised-learning system that allows, based on teaching examples and the applied learning algorithms, to associate the feature vectors constituting its input with the class label. Learning classifier systems are used in many areas to process very large data resources and automate the inference process. It is impossible to fully review the specific applications of these systems or even to mention all their application areas. In the context of this article, it is noteworthy to mention the area of road roughness classification [22], intelligent fault diagnosis of rotating machinery [23] or detection of damage to rolling bearings [24].

Learning classifier systems are also used in the diagnostics of the track and turnouts, for example, see [25–27]. One way to identify a class is to use deep learning methods. Here, a CNN can be proposed. CNNs are particularly useful in image and speech recognition but, more generally, in classification processes.

Such a network, in various configurations, performs better in many cases compared to other solutions. It is the result of research on the visual cortex [28, 29]. The most important component of a CNN is a convolutional layer. The idea behind such a layer is that its neurons connect to only a small number of the previous layer's neurons (the receptive field). As a result, teaching such a network is much faster and more effective than in the case of networks in which neurons are fully connected. The weights of the neuron in the convolution layer are filters that emphasise specific elementary features of the image. Thanks to the use of a particular filter, a specific map of features is obtained. Different filters are used to create a whole stack of feature maps.

Map of layer features l is calculated as [30]:

$$(2.1) \qquad \mathbf{x}_j^l = f\left(\sum_d \mathbf{k}_{jd}^l * \mathbf{x}_d^{l-1} + \mathbf{b}_j^l\right),$$

where l is network layer, $\mathbf{x}_d^{l-1}$ is d-th vector of features in layer $l-1$, $\mathbf{x}_j^l$ is j-th vector of features in layer l, $\mathbf{k}$ is a convolution kernel, $\mathbf{b}$ is bias vector, and f is activation function.

In CNNs, the rectified linear unit (ReLU) activation function can be used [28]:

$$(2.2) \qquad f(x) = \begin{cases} x, & x \geq 0, \\ 0, & x < 0. \end{cases}$$

Another layer that can often be found in CNN is a pooling layer. Its purpose is to subsample the input image in order to reduce both the risk of overtraining and computational load. This is done by collecting input data using a specific aggregate function (such as max or mean). Normalisation is often performed between the convolution layer and the ReLU layer, which speeds up training and reduces the sensitivity to initialisation values of the network weights. All these layers can be used many times in the network.

The last part of the CNN are, as a rule, fully connected layers creating a supervised learning classifier implemented in the form of a neural network with a softmax function as an output. The output of a fully connected layer can be expressed as:

$$(2.3) \qquad \mathbf{x}^l = g\left((\mathbf{w}^l)^{\mathrm{T}}\mathbf{x}^{l-1} + \mathbf{b}^l\right),$$

where l is network layer, $\mathbf{x}^{l-1}$ is output of layer $l-1$, $\mathbf{x}^l_j$ is output of layer l, $\mathbf{w}^l$ is fully connected layer weight matrix, $\mathbf{b}$ is bias vector, and g is activation function.

The softmax function calculates for each neuron of the last fully connected layer the probability that the network input vector belongs to a specific class [31]:

$$(2.4) \qquad p_c = \frac{\exp\left((\mathbf{w}^L_c)^{\mathrm{T}}\mathbf{x}^{L-1}\right)}{\sum\limits_{c=1}^{C} \exp\left((\mathbf{w}^L_c)^{\mathrm{T}}\mathbf{x}^{L-1}\right)},$$

where p_c is the probability that the example $\mathbf{x}$ belongs to the class c, L is the last layer of the CNN, $\mathbf{x}^{L-1}$ is the output of layer $L-1$, $\mathbf{w}$ is vector of weights, and C is number of classes.

The above expression allows to determine the loss function E:

$$(2.5) \qquad E = -\frac{1}{m}\sum_{i=1}^{m}\sum_{c=1}^{C} y_{c,i}\log(p_c),$$

where m is number of teaching examples, $y_{c,i}$ is equal to 1 if c is the target class for i-th example, and 0 otherwise.

Network learning algorithms minimise the loss function. The trained network allows for the process of classifying the input feature vectors to take place.

Due to the considerable effectiveness of convolutional networks in recognising images, it was decided to use them in identifying the occurrence of rail corrugation.

3. Research methodology

In order to obtain training and test examples, 35 available recordings of a low-floor tram ride through various measurement sections were used. The locations of corrugation were known.

For the analysis, the vibration acceleration signal from one of the sensors (Brüel & Kjaer type 4504) placed on the wheelset of the tram (on the right and left axle box), measured in the vertical direction (perpendicular to the vehicle axis), was selected. Both rails were affected by the corrugation in the measurement section. The sound pressure was also used, measured with two microphones (Brüel & Kjaer 4189-A-021) attached under the vehicle near the first wheelset, on its left-hand and right-hand sides.

Additionally, the value of the averaged vehicle speed was determined based on the spectral analysis of the signal obtained from a tachometer, which generated an impulse with every rotation of the wheel. The measurement data acquisition was carried out using a 17-channel Brüel & Kjaer 3560-C acquisition module. Signals were recorded synchronously in all measurement channels. The signals were initially recorded with a frequency of approx. 65.5 kHz. Such a wide range of recording was chosen as it was planned to use the results in many other studies. Archiving recorded signals in digital form was done directly on a laptop computer. Prior to the measurements, the measurement path was calibrated.

In Fig. 2, examples of short-time Fourier transform analyses for the cases of occurrence and absence of corrugation are presented. The analyses are performed on fragments of the original recording of vibration accelerations on the wheelset of the tram in the vertical direction (perpendicular to the track) and narrowed in the frequency and time domains.

As shown in Fig. 2, the detection of corrugation in some cases is not trivial and must be based on an analysis of a sufficiently long signal fragment in frequency bands in order to average the appropriate measures.

Due to the occurrence of the signs of the corrugation phenomenon in low frequencies, the band was narrowed down to approx. 500 Hz, which was obtained by filtering with a non-recursive filter and signal decimation. The high-pass filtration above 10 Hz was also performed with the Butterworth filter due to the presence of very significant vibrations in the band below the cut-off frequency in all analysed recordings, regardless of the presence or absence of corrugation. This narrowed the scope of the possibility of detecting the phenomenon of long-wavelength corrugation; however, it allowed to partially remove the components
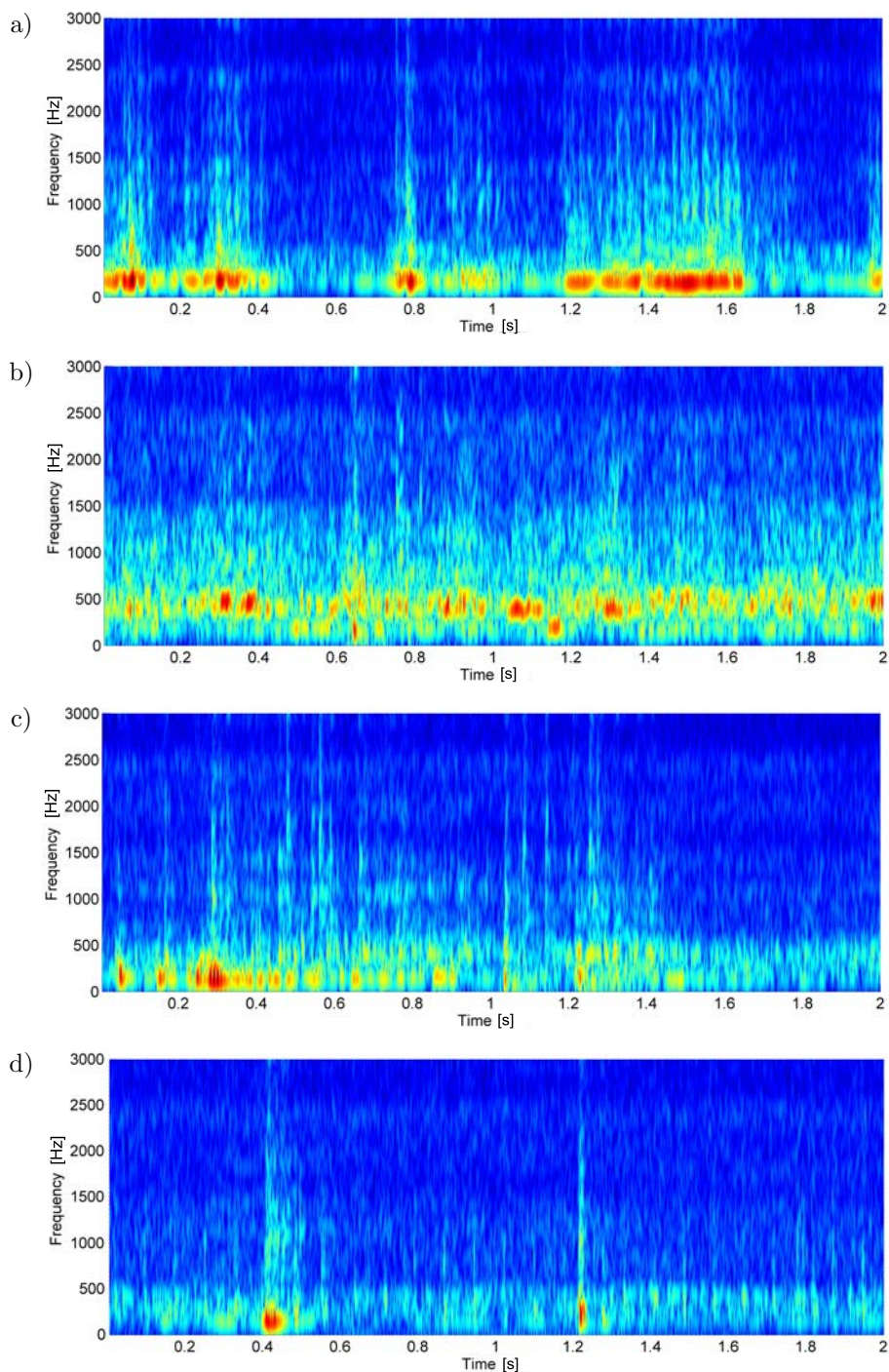
FIG. 2. Results of short-time Fourier transform analyses for the case of corrugation (a) and different track sections without corrugation (b), (c), (d).

originating from completely different inputs than those sought. Of course, it should be remembered that the generated vibration frequencies depend not only on the wavelength but also on the travel speed.

In order to generate the appropriate number of training examples needed to train and test classifiers, each recording was divided into smaller time sections of 2.5 s. The length of the section was selected arbitrarily. Based on the obtained fragments, point measurements of signals were determined. These were root-mean square (RMS) values in five separate frequency bands for each of the four measurement channels. Each band was approx. 50 Hz wide (after taking into account the high-pass filtration, the first band effectively covered the range of approx. 40 Hz). The highest band covered the range from approx. 200 Hz to approx. 250 Hz. Due to the nature of the generation of the phenomenon, appropriate excitation should be expected exactly in these bands (depending on the wavelength and speed of travel). Unfortunately, often other phenomena unrelated to corrugation may also occur in the same bands. Hence, other measures in the range up to about 500 Hz were also taken into account: kurtosis, skewness, impulse, crest, waveform and clearance factors. These measures were calculated for both acceleration signals and sound pressure.

Additionally, the vehicle speed was taken into account at the classifier input. There were relatively few sections where the presence of corrugation was found by visual observation. In order to check the effectiveness of detecting corrugation, many registrations of various types of substructure as well as crossings were used for which no corrugation was found. Table 1 shows how many examples were obtained in each set.

Table 1. The cardinality of subsets with examples.

Class	The cardinality of learning sets
Positive – with corrugation	617
Negative – without corrugation	22565
Total	23182

Table 1 shows that the positive class is sparse and poorly represented in relation to the alternative class. For this reason, the weighted percentage error was used to assess the classification error, expressed by the formula:

$$(3.1) \qquad \varepsilon = \frac{100}{K} \sum_{i=1}^{K} \frac{\sum_{j=1, j \neq i}^{K_i} a_{ij}}{K_i},$$

where K is number of classes, K_i is number of elements in i-th class, and a_{ij} are elements of the class distribution matrix (error matrix) outside the diagonal.

4. Results and discussion

Figure 3 shows exemplary (randomly selected) components of the attribute vector relating to vibration accelerations measured on the right-hand side of the vehicle, which were normalised to the maximum value for the sections with corrugation (Fig. 3a) and sections where no corrugation was found (Fig. 3b). The first value presented in Fig. 3 is the normalised speed, the next are the effective
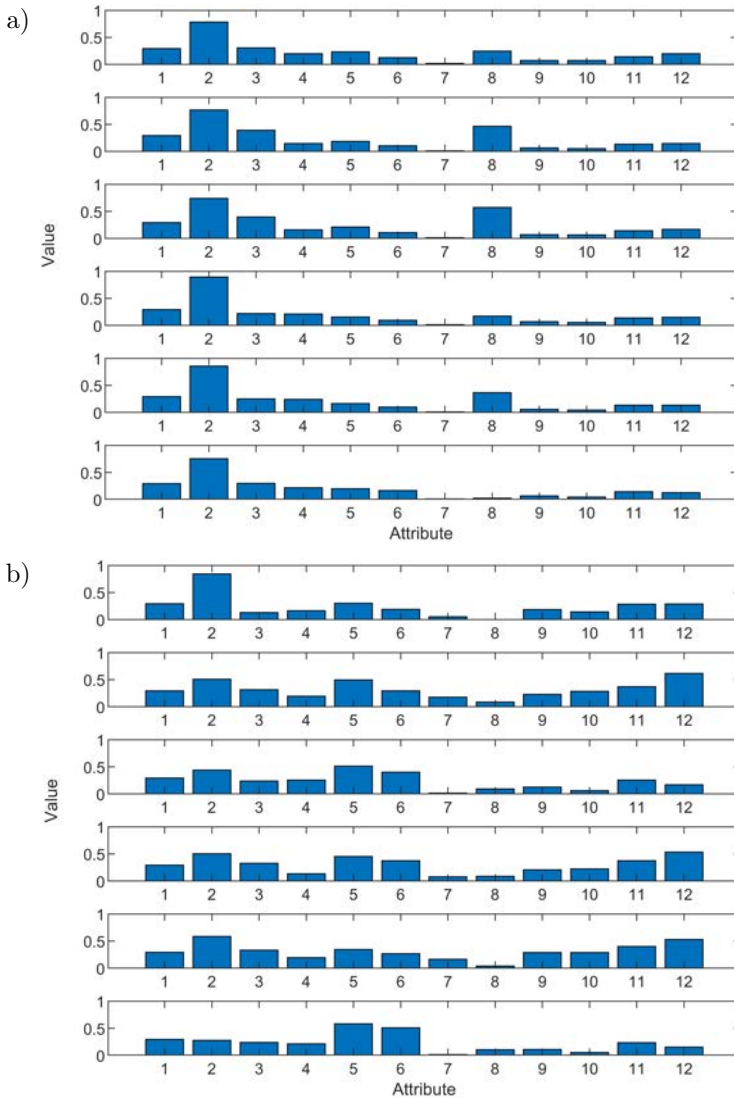

Fig. 3. Comparison of the vectors of acceleration signal measures from the sensor on the right-hand side of the vehicle for the randomly selected fragments of signals obtained: a) from sections with corrugation, b) from sections without corrugation.

values in five bands followed by kurtosis, skewness, as well as factors of impulse, crest, waveform and clearance. From the exemplary figures and the analysis of data from a larger sample, it can be concluded that the identification of corrugation on the basis of single measures for the data under consideration may not be possible, and only an appropriate combination of these measures may reduce the recognition error. This is due to the fact that in many cases, the measurements that are sensitive to the occurrence of corrugation (e.g., RMS value in the band up to approx. 50 Hz) are also sensitive to the occurrence of other phenomena. Additionally, it is important to use information from both sides of the vehicle, as certain phenomena (e.g., rail crack) may occur on just one of them, which hinders the correct classification.

In order to solve the problem, a classifier based on convolutional networks was chosen, as it is specialised in image recognition. Three variants were taken into consideration: vibration acceleration signals only, solely acoustic pressure signals, and both pressure and vibration signals simultaneously. Such an analysis made it possible to determine whether one of the measurements could be eliminated in order to simplify the corrugation detection system.

For each of the aforementioned input data sets, the network was independently configured by running multiple simulations to find the optimal network structure. The structure of the convolutional network was selected using the simplification method, comparing test errors expressing the inability of the network to generalise the learned knowledge. Testing was conducted based on a hold-out test, whereas 70% of the data were randomly selected for training and 30% of the available examples were selected for testing. Such an assessment of a testing error has the potential to inflate its value [32]. The tests were repeated 30 times for each method.

The optimization of the network structure was carried out with regard to the selection of the number of neurons in the convolution layers and the softmax network layer. The kernel size was chosen arbitrarily to reduce the number of parameters supplied.

An example of the results of the classification error for the test set for different network structures is shown in Fig. 4. This figure concerns the set of vibration and sound pressure data considered jointly and two convolutionary layers of the network. The number of neurons in the first layer of the softmax network was marked with N. The output layer always contained two neurons (identification of one of the two classes). The parameters n and m denote the numbers of filters in both convolutional layers, respectively. It was assumed that the number of filters in the first layer is smaller than in the second (for networks with two layers), in accordance with the frequently used principle [28]. In order to reduce the number of parameters, the number of filters in the second layer was twice as large as in the first.
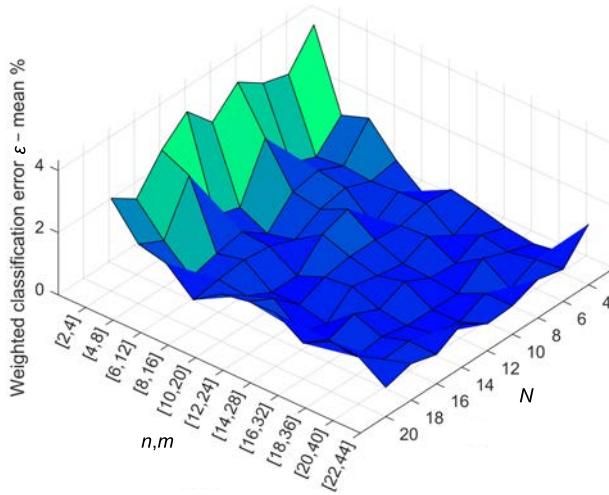
FIG. 4. Influence of the network structure selection on the obtained classification errors.

The network weights were selected randomly, so the learning was carried out many times to reduce the impact of the initial weight values on the results. Of course, a repetition of 30 times may turn out to be too small to eliminate such an impact. However, the optimization of the network structure (although it does not ensure the global minimum classification error) allowed for the selection of the structure with an acceptable error.

Further attempts were also made by adding another layer of the convolutional network, but no improvement in the quality of the classification was achieved.

Based on the obtained results, the standard deviation was also calculated, which allowed to assess the estimated stability of the classification error for a given network. A diagram of the final form of the network, taking into account both vibrations and acoustic pressure, is presented in Fig. 5.
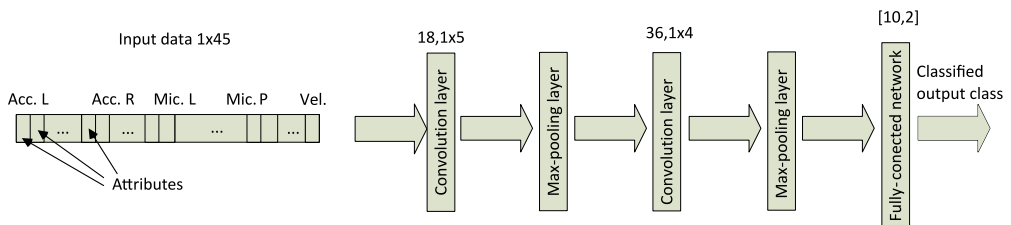

FIG. 5. The structure of the convolutional network used to detect the phenomenon of rail corrugation in the version that takes into account accelerometers and acoustic pressures (Acc – accelerometers, Mic – microphone, L – left-hand and R – right-hand side, Vel – velocity).

Before the learning process, the effective values were normalised by relating them to the maximum values obtained in the data set. The input layer of the

network was an "image" composed of the vectors of the previously described measures. In the final version, including vibration acceleration, sound pressure and speed, a vector with 45 elements was fed to the network input.

The first convolutional layer in the network proposed in Fig. 4 was composed of 18 filters (convolution kernels). The kernel in the first convolution layer was 1×5 in size. The non-linear activation function ReLU defined by Eq. (2.2) was used. Before the next convolution layer, a max-pooling layer with a dimension of pooling region equal to 1×4 was used. From areas of this dimension, the maximum value was determined. Because the step size for traversing input was 1, pooling regions overlap. The next convolution layer was built of 36 filters with a size of 1×4. After this layer, another max-pooling layer with a dimension of pooling region equal to 1×2 was used. The last layers of the network were layers of the classical pattern recognition neural network with two fully connected neuron layers of 10 and 2 neurons in size, respectively, and with a softmax layer at the output. For the cases with only vibrations or only sound taken into consideration, the network structure was simpler, although it also required two convolutional layers.

Table 2 shows the best results for various network structures obtained on separate test sets, assessed using the error described by Eq. (3.1), with 30 averages obtained by a hold-out test.

Table 2. Summary of the total classification error – the best average results obtained.

Variant	Input measures included	Weighted classification error ε – mean [%]	Standard deviation of error [%]
1	Only vibration accelerations	3.04	2.07
2	Only sound pressure	2.58	2.21
3	Sound pressure and vibration acceleration combined	0.50	0.64

The analysis of the results shows that the best results can be obtained using both vibrations and sound (variant 3). Taking these values into account at the same time allows to obtain negligible identification errors. Presumably, if all channels are taken into account, it increases the resistance to interferences that may occur temporarily on some of the channels. Table 2 also shows that the results of the test error for variants 1 and 2 do not differ significantly, and the errors obtained are also at an acceptable level in each of the considered cases. Taking into account the fact that the diagnostic system mounted on the vehicle may cover the same track section many times – which should increase the accuracy of the final classification – it seems that such a system can be built based on two measuring microphones or alternatively two vibration acceleration sensors. The CNN made it possible to achieve a very small classification error, although its

training, and especially the selection of the network structure, requires a long time. However, the learned network can operate in real time, constituting the basis for building a diagnostic system. It is also important to observe that further simplification of the system, e.g., by leaving only one of the channels, meant that the errors obtained were much higher (in the order of 8÷10%), which indicates that measurements on both sides of the vehicle are necessary. This may be due to the occurrence of vibration or acoustic phenomena, for example masking the occurrence of corrugation on one side of the vehicle at the given moment. Moreover, in the case of a theoretical situation when corrugation appears on only one of the rails, it might not be possible to detect such a state.

5. Conclusions

As a result of the conducted analyses, it is possible to propose a system for identifying the occurrence of rail corrugation. The proposed system can be based on two microphones or two unidirectional vibration acceleration sensors mounted on a wheelset. This solution allows to achieve corrugation detection with errors that are fully acceptable. As shown, taking into account signals both from microphones and accelerometers, the presented method allows to obtain classification errors of 1%. It can be assumed that when considering multiple runs of a tram equipped with the measuring system, the expected classification error may be further reduced. The required measurement bandwidth covers the range of low frequencies (up to approx. 500 Hz), and the measures used are very simple to calculate. The multi-channel recording of signals with a relatively low sampling frequency does not cause data collection problems. As shown, a CNN with a simple architecture is very suitable for data analysis. However, the process of building such a classifier is very time-consuming. The presented results concern the best network structures among many considered, therefore, optimising the network structure is not of a global nature. The obtained error may be even smaller than the presented one.

Acknowledgments

References

1. EN 13231-3:2012, *Railway applications. Track. Acceptance of works. Acceptance of repro-filing rails in track.*

2. Bednarek W., Railroad corrugation (causes and countermeasures) [in Polish: Zużycie faliste szyn toru kolejowego (przyczyny i środki zaradcze)], *Archiwum Instytutu Inżynierii Lądowej*, (2015): 7–23, 2015.

3. GRASSIE S.L., Corrugation on Australian National: cause, measurement and rectification, [in:] *Proceedings of the Fourth International Heavy Haul Railway Conference 1989: Railways in Action*, Brisbane, Australia, pp. 188–192, 1989.

4. OOSTERMEIJER K.H., Review on short pitch rail corrugation studies, *Wear*, **265**(9–10): 1231–1237, 2008, doi: 10.1016/j.wear.2008.01.037.

5. GRASSIE S.L., Corrugation: variations on an enigma, *Railway Gazette International*, **146**(7): 531–533, 1990.

6. GRASSIE S.L., KALOUSEK J., Rail corrugation: characteristics, causes and treatments, *Proceedings of the Institution of Mechanical Engineers, Part F: Journal of Rail and Rapid Transit*, **207**(1): 57–68, 1993, doi: 10.1243/PIME_PROC_1993_207_227_02.

7. GRASSIE S.L., Rail corrugation: advances in measurement, understanding and treatment, *Wear*, **258**(7–8): 1224–1234, 2005, doi: 10.1016/j.wear.2004.03.066.

8. GRASSIE S.L., Rail corrugation: characteristics, causes, and treatments, *Proceedings of the Institution of Mechanical Engineers, Part F: Journal of Rail and Rapid Transit*, **223**(6): 581–596, 2009, doi: 10.1243/09544097JRRT264.

9. SATO Y., MATSUMOTO A., KNOTHE K., Review on rail corrugation studies, *Wear*, **253**(1–2): 130–139, 2002, doi: 10.1016/S0043-1648(02)00092-3.

10. ISHIDA M., MOTO T., TAKIKAWA M., The effect of lateral creepage force on rail corrugation on low rail at sharp curves, *Wear*, **253**(1–2): 172–177, 2002, doi: 10.1016/S0043-1648(02)00096-0.

11. SUDA Y., HANAWA M., OKUMURA M., IWASA T., Study on rail corrugation in sharp curves of commuter line, *Wear*, **253**(1–2): 193–198, 2002, doi: 10.1016/S0043-1648(02)00099-6.

12. LIU Q.Y., ZHANG B., ZHOU Z.R., An experimental study of rail corrugation, *Wear*, **255**(7–12): 1121–1126, 2003, doi: 10.1016/S0043-1648(03)00213-8.

13. FINK M., The emergence of the rail corrugation; The status of corrugation research after around 60 years [in German: Die Entstehung der Schienriffeln; Der Stand der Riffelforschung nach rund 60 Jahren] (part 1 of 2), *Glasers Annalen*, No. 11: 342–350, 1953.

14. WEI X., YIN X., HU Y., HE Y., JIA L., Squats and corrugation detection of railway track based on time-frequency analysis by using bogie acceleration measurements, *Vehicle System Dynamics*, **58**(8): 1167–1188, 2020, doi: 10.1080/00423114.2019.1610181.

15. LANG K., XING Z., DONG W., GAO X., A rail corrugation detection method based on wavelet packet energy entropy, [in:] Jia L., Qin Y., Suo J., Feng J., Diao L., An M. [Eds.], *Proceedings of the 3rd International Conference on Electrical and Information Technologies for Rail Transportation (EITRT) 2017. EITRT 2017. Lecture Notes in Electrical Engineering*, vol. 483, Springer, Singapore, 2018, doi: 10.1007/978-981-10-7989-4_21.

16. LI J., SHI H., Rail corrugation detection of high-speed railway using wheel dynamic responses, *Shock and Vibration*, **2019**: Article ID 2695647, 12 pages, 2019, doi: 10.1155/2019/2695647.

17. ZHANG H., WANG N., LIU S., LI B., Rail corrugation identification method based on parameter optimization VMD and SPWVD, *Railway Computer Application*, **29**(6): 18–24, 2020.

18. XIAO B., LIU J., ZHANG Z., A heavy-haul railway corrugation diagnosis method based on WPD-ASTFT and SVM, *Shock and Vibration*, **2022**: Article ID 8370796, 14 pages, 2022, doi: 10.1155/2022/8370796.

19. KANG G., LI C., QIN L., Rail corrugation detection method based on laser imaging technology, *Urban Mass Transit*, **10**(181): 94–97+111, 2017.

20. LI P., WANG P., CHEN P., Rail corrugation detection based on 3D structured light and wavelet analysis, *Railway Standard Design*, **062**(008): 33–38, 2018.

21. FENG J.H., YUAN H., HU Y.Q., LIN J., LIU S.W., LUO X., Research on deep learning method for rail surface defect detection, *IET Electrical Systems in Transportation*, **10**(4): 436–442, 2020, doi: 10.1049/iet-est.2020.0041.

22. GORGES C., ÖZTÜRK K., LIEBICH R., Impact detection using a machine learning approach and experimental road roughness classification, *Mechanical Systems and Signal Processing*, **117**: 738–756, 2019, doi: 10.1016/j.ymssp.2018.07.043.

23. LEI Y., HE Z., ZI Y., Application of an intelligent classification method to mechanical fault diagnosis, *Expert Systems with Applications*, **36**(6): 9941–9948, 2009, doi: 10.1016/j.eswa.2009.01.065.

24. MECHEFSKE C.K., MATHEW J., Fault detection and diagnosis in low speed rolling element bearings Part II: The use of nearest neighbour classification, *Mechanical Systems and Signal Processing*, **6**(4): 309–316, 1992, doi: 10.1016/0888-3270(92)90033-F.

25. FIRLIK B., TABASZEWSKI M., Monitoring of the technical condition of tracks based on machine learning, *Proceedings of the Institution of Mechanical Engineers, Part F: Journal of Rail and Rapid Transit*, **234**(7): 702–708, 2020, doi: 10.1177/0954409719866368.

26. TSUNASHIMA H., Condition monitoring of railway tracks from car-body vibration using a machine learning technique, *Applied Sciences*, **9**(13): 27–34, 2019, doi: 10.3390/app9132734.

27. SYSYN M., GRUEN D., GERBER U., NABOCHENKO O., KOVALCHUK V., Turnout monitoring with vehicle based inertial measurements of operational trains: a machine learning approach, *Communications – Scientific Letters of the University of Zilina*, **21**(1): 42–48, 2019, doi: 10.26552/com.C.2019.1.42-48.

28. GÉRON A., *Hands-on Machine Learning with Scikit-Learn, Keras and TensorFlow*, O'Reilly Media, 2017.

29. SARKER G., Some studies on convolution neural network, *International Journal of Computer Applications*, **182**(21): 13–22, 2018, doi: 10.5120/ijca2018917965.

30. CHEN R., HUANG X., YANG L., XU X., ZHANG X., ZHANG Y., Intelligent fault diagnosis method of planetary gearboxes based on convolution neural network and discrete wavelet transform, *Computers in Industry*, **106**: 48–59, 2019, doi: 10.1016/j.compind.2018.11.003.

31. JIA F., LEI Y., LU N., XING S., Deep normalized convolutional neural network for imbalanced fault classification of machinery and its understanding via visualization, *Mechanical Systems and Signal Processing*, **110**: 349–367, 2018, doi: 10.1016/j.ymssp.2018.03.025.

32. KORBICZ J., KOŚCIELNY J.M., KOWALCZUK Z., CHOLEWA W., *Fault Diagnosis: Models, Artificial Intelligence, Applications*, Springer Science & Business Media, Berlin Heidelberg, 2004, doi: 10.1007/978-3-642-18615-8.